HHS Public Access

Author manuscript

Epilepsia. Author manuscript; available in PMC 2021 November 01.

Published in final edited form as:

Epilepsia. 2020 November ; 61(11): 2534–2544. doi:10.1111/epi.16686.

Seizure-onset regions demonstrate high inward directed connectivity during resting-state: An SEEG study in focal epilepsy

Saramati Narasimhan[1,2,3], **Keshav B. Kundassery**[2], **Kanupriya Gupta**[1,2], **Graham W. Johnson**[2,3], **Kristin E. Wills**[1,2], **Sarah E. Goodale**[2,3], **Kevin Haas**[4], **John D. Rolston**[5], **Robert P. Naftel**[1], **Victoria L. Morgan**[1,2,3,6], **Benoit M. Dawant**[3,7], **Hernán F. J. González**[2,3], **Dario J. Englot**[1,2,3,6,7]

[1]Department of Neurological Surgery, Vanderbilt University Medical Center, Nashville, Tennessee

[2]Department of Vanderbilt University Institute of Imaging Science, Vanderbilt University Medical Center, Nashville, Tennessee

[3]Department of Biomedical Engineering, Vanderbilt University, Nashville, Tennessee

[4]Department of Neurology, Vanderbilt University Medical Center, Nashville, Tennessee

[5]Department of Neurosurgery, University of Utah, Salt Lake City, Utah

[6]Department of Radiology and Radiological Sciences, Vanderbilt University Medical Center, Nashville, Tennessee

[7]Department of Electrical Engineering and Computer Science, Vanderbilt University, Nashville, Tennessee

Abstract

Objective: In patients with medically refractory focal epilepsy, stereotactic-electro-encephalography (SEEG) can aid in localizing epileptogenic regions for surgical treatment. SEEG, however, requires long hospitalizations to record seizures, and ictal interpretation can be incomplete or inaccurate. Our recent work showed that non-directed resting-state analyses may identify brain regions as epileptogenic or uninvolved. Our present objective is to map epileptogenic networks in greater detail and more accurately identify seizure-onset regions using directed resting-state SEEG connectivity.

Methods: In 25 patients with focal epilepsy who underwent SEEG, 2 minutes of resting-state, artifact-free, SEEG data were selected and functional connectivity was estimated. Using standard clinical interpretation, brain regions were classified into four categories: ictogenic, early

Correspondence: Saramati Narasimhan, Department of Neurological Surgery, Vanderbilt University Medical Center, 1500 21st Avenue South, VAV 4340, Nashville 37212, Tennessee. saramati.narasimhan.1@vumc.org.

CONFLICTS OF INTEREST

None of the authors has any conflict of interest to disclose. We confirm that we have read the Journal's position on issues involved in ethical publication and affirm that this report is consistent with those guidelines.

ETHICAL APPROVAL

We confirm that we have read the Journal's position on issues involved in ethical publication and affirm that this report is consistent with those guidelines.

propagation, irritative, or uninvolved. Three non-directed connectivity measures (mutual information [MI] strength, and imaginary coherence between and within regions) and four directed measures (partial directed coherence [PDC] and directed transfer function [DTF], inward and outward strength) were calculated. Logistic regression was used to generate a predictive model of ictogenicity.

Results: Ictogenic regions had the highest and uninvolved regions had the lowest MI strength. Although both PDC and DTF inward strengths were highest in ictogenic regions, outward strengths did not differ among categories. A model incorporating directed and nondirected connectivity measures demonstrated an area under the receiver-operating characteristic (ROC) curve (AUC) of 0.88 in predicting ictogenicity of individual regions. The AUC of this model was 0.93 when restricted to patients with favorable postsurgical seizure outcomes.

Significance: Directed connectivity measures may help identify epileptogenic networks without requiring ictal recordings. Greater inward but not outward connectivity in ictogenic regions at rest may represent broad inhibitory input to prevent seizure generation.

Keywords

focal epilepsy; functional connectivity; intracranial EEG; localization; prediction

1 | INTRODUCTION

Epilepsy affects approximately 50 million persons worldwide, with one-third of patients resistant to anti-epileptic medications.[1] Fortunately, many patients with medically refractory focal epilepsy may be surgical candidates.[2] Favorable surgical outcomes rely on accurate identification of seizure-onset and propagation networks.[3] Stereo-electroencephalography (SEEG) is a minimally invasive method used to identify regions for surgical intervention, using intracerebral electrodes to measure ictal/interictal brain activity.[4,5] Recently SEEG utilization has increased rapidly outside Europe.[6–8] After SEEG implantation, patients are monitored in the hospital for days/weeks, often using medication wean, sleep deprivation, electrical stimulation, and/or other interventions to induce seizures. Potential limitations include incomplete/inaccurate interpretation of ictal origin, failure to capture all seizure types, triggering atypical seizure types, and prolonged hospitalizations.[9,10] Resting-state network analysis methods may supplement clinical interpretation by defining epileptogenic networks without requiring ictal recordings, and methods are currently being explored.[11–14]

We recently analyzed resting-state SEEG in a small cohort, using alpha-band imaginary coherence to estimate functional connectivity.[15] We found that epileptogenic structures demonstrated higher connectivity than nonepileptogenic regions, and connectivity measures may predict epileptogenicity with modest accuracy.[15] Beyond small sample size, one limitation is that information may be lost using dichotomized regional classification, without considering other areas involved in seizure networks.[14,16] Although imaginary coherence is a linear measurement,[17] it is unknown if nonlinear, information theorybased connectivity may demonstrate improved accuracy in identifying epileptogenic regions. Furthermore, it is unclear if higher connectivity at epileptogenic regions is inward and/or outward, and if directed connectivity measurements may improve our ability to predict epileptogenicity.[15]

The present study builds upon our prior study,[15] and now seeks to better characterize both nondirected and directed connectivity in regions throughout the epilepsy network using brief, resting-state SEEG recordings in patients with focal epilepsy. We will evaluate differences between ictogenic, early propagation, irritative, and uninvolved brain regions. Ultimately, we aim to optimize resting-state SEEG connectivity measures to help accurately identify surgical targets, supplement traditional clinical interpretation, and improve patient care.

2 | METHODS

2.1 | Subjects

Twenty-five patients with medically refractory focal epilepsy were included in this study, including 15 individuals from our prior study.[15] Patients had video monitoring and SEEG recordings obtained at Vanderbilt University Medical Center (VUMC) between 2017 and 2019. This investigation was approved by VUMC Institutional Review Board, and informed written consent was obtained from patients. Demographics and characteristics were recorded by the treating epileptologists (Table 1). Following these recordings, at the time of analyses, 22 patients received surgical epilepsy treatment. Three patients either declined surgical therapy or were pending scheduling. Postoperative seizure outcome was determined at last follow-up for 21 patients who had ≥12 months of follow-up. Outcomes were assessed using Engel classification scale[18] for patients who received resection, or percent decrease in seizure frequency for individuals who underwent responsive neurostimulation (RNS) placement.

2.2 | Data collection and preprocessing

Electrode trajectories were planned by treating physicians according to standard clinical care at VUMC using CRAnialVault Explorer (CRAVE; Vanderbilt University, Nashville, Tennessee).[19] SEEG electrodes (Ad-Tech, or PMT Corporation) were implanted using stereotactic technique (Table 1). A JE-209 clinical EEG system (Nihon Kohden America) or Quantum Amplifier EEG system (Natus) was used to record 20 minutes of interictal data at a sampling rate of 0.5 or 1 kHz (all data was band-pass filtered 1–119 Hz, below Nyquist frequency, prior to analyses). Recordings occurred during eyes-closed resting-state, defined by Raichle.[20]

As in our prior work, raw SEEG data were preprocessed.[15] Raw signal was band-pass filtered (1–119 Hz) and notch filtered (60 Hz) in EEGLab (https://sccn.ucsd.edu/eeglab/index.php). Anatomical magnetic resonance imaging (MRI) registered with computerized tomography (CT) post-implantation of SEEG with CRAVE was used to exclude electrode contacts outside the brain, completely in white matter, or in cerebrospinal fluid. Anatomical location of remaining electrodes in gray matter was assigned using Harvard-Oxford Atlas (Harvard Center of Morphometric Analysis). Channels with artifacts were removed.[21] Per patient, we identified a continuous 120-second segment of resting-state SEEG data for analysis. A 2-minute data segment was chosen to be long enough for stable functional connectivity measurements, yet short enough to avoid artifacts/interictal spikes. In previous SEEG work,[15] we compared 2, 5, and 10-minute data segments and observed similar

connectivity results. In addition, EEG connectivity analyses by others have demonstrated stability of various functional networks using 2-minute data segments,[22] and magnetoencephalography (MEG) connectivity analysis using similar measure also reveal that 1–2 minute data segments can be used to produce reliable connectivity results.[23]

All connectivity analysis was performed on 25, 2-minute segments, with one segment used per patient. All connectivity analyses were performed on the entirety of the 2-minute segment. Using FieldTrip MATLAB toolbox (http://www.fieldtriptoolbox.org/), electrodes were referenced with bipolar montage.[24] Therefore, all connectivity metrics were calculated on electrode contact pairs. Although overlapping pairs within a region were used, contact pairs straddling two regions were excluded from analysis.

Epileptogenicity of brain regions sampled by SEEG was classified using all clinical SEEG, prior to connectivity analysis. Two classification schemes were used. We first used a binary classification method where regions were labeled as epileptogenic or non-epileptogenic.[15] This designation was based on Luders and colleagues.[25,26] We utilized a four-category classification scheme to evaluate epileptic network in greater detail, and other recent groups have also designated nonbinary classifications.[11] Bartolomei et al[27] referred to epileptic, propagation, and noninvolved networks. Here, we classified regions as ictogenic, early propagation, irritative, or uninvolved. Areas of clear seizure onset were considered ictogenic. Early propagation regions demonstrated rapid spread of ictal activity within ~10 seconds of seizure onset, and are often targeted surgically when safe.[3] Structures where interictal epileptiform spike activity was noted, but did not demonstrate ictal onset or rapid spread, were labeled as irritative. All other brain regions were classified as uninvolved.

2.3 | Functional connectivity measurements

Three nondirected measurements were calculated from resting-state SEEG, including mutual information (MI) strength and two measures based on alpha-band imaginary coherence. Unlike coherence, MI does not assume data linearity.[28,29] MI is derived from information theory; MI quantifies to what extent uncertainty about a given stimulus is reduced by accounting for a single trial of a neural response. Generally, MI quantifies shared dependence between two signals. MI was calculated using FieldTrip per electrode contact pair using all frequency bands using Direct Method to avoid assuming probability distribution shape,[28] and quadratic extrapolation was used as bias correction. MI strength was calculated across electrode contact pairs, and then averaged across electrode contact pairs within each brain region per patient. Three-dimensional representations of MI strength in individual patients were visualized using BrainNet Viewer.[30]

We also calculated two nondirected measures based on imaginary coherence. We defined “within” imaginary coherence as mean alpha-band (8–12 Hz) imaginary coherence of electrode contact pairs within a brain region to other electrode contact pairs within the same region.[15] Conversely, we defined “between” imaginary coherence as mean alpha-band imaginary coherence between electrode contact pairs in a given brain structure and electrode contact pairs in all other areas sampled. Unlike coherence, imaginary coherence analysis minimizes artifact/volume conduction effects by ignoring zero-time lag signals.[31] In addition, test-retest reliability for imaginary coherence is high in alpha-band, likely due to

alpha EEG peak in awake resting-state.[11] In our previous study, we measured connectivity in delta, theta, and alpha bands, and found that connectivity differences in epileptogenic regions were present in all bands, but most prominent in alpha-band.[15] Thus we focused on alpha-band here.

To evaluate directed connectivity, we measured partial directed coherence (PDC) and directed transfer function (DTF) in alpha-band. These measures have been utilized in previous electrographic studies of human epilepsy networks.[32–35] Both PDC and DTF are based on Granger causality prediction modeling, which evaluates the ability to predict a time-varying signal based on previous information in another time-varying signal.[36,37] When prior values of one signal improve prediction of a second signal beyond prior values of the second signal alone, the temporal precedence infers causality. According to their mathematical definitions, PDC is rescaled with respect to the region that sends a signal, whereas DTF is rescaled with respect to the region that receives a signal.[37] Both metrics are relatively resistant to volume-conduction influences.[36] Because multiple time series were evaluated per patient, a multivariate autoregression model was first performed on preprocessed SEEG data with an order of 10. This order was selected based on results of a previous investigation that evaluated multiple multivariate models with orders between 2 and 22,[38] and 10 is also the recommended FieldTrip default. Then inward and outward strengths for both PDC and DTF were calculated per electrode contact pair. Final values of MI, PDC, and DTF strengths were normalized within each patient. Electrode contact pair strengths were averaged per brain region per patient.

2.4 | Statistical analyses and modeling

We used the Anderson-Darling test to determine if connectivity values were normally distributed prior to utilizing parametric statistical tests. Connectivity values across all metrics in all region types were found to be normally distributed, so parametric statistical tests were used.

To compare connectivity measures in epileptogenic vs nonepileptogenic regions across all patients, we used paired-sample *t* tests (*t* = test statistic value, *df* = degrees of freedom). To evaluate connectivity differences across region types using four-category regional classification scheme—ictogenic, early propagation, irritative, and uninvolved—we used ANOVA (*df* = total degrees of freedom, *F* = *F*-statistic). To avoid oversampling, we calculated mean connectivity of all regions in each category for each patient prior to statistical testing (ie, n = 25 patients, not regions, for statistical tests).

We also sought to generate a model to predict ictogenicity of individual brain regions using combined directed and non-directed connectivity measures. This analysis was performed using binary classification logistic regression. Regions were classified as ictogenic or not ictogenic, with the latter category including early propagation, irritative, and uninvolved areas. Sensitivity and specificity measures signify the model's ability to predict ictogenicity of a brain region. Five measures incorporated into the model included between and within imaginary coherence, MI strength, and inward PDC and DTF strength. These variables were chosen for the multivariate regression model based on results of univariate testing, as these connectivity measures were significantly different in ictogenic regions ($P < .05$, after

correction). Receiver-operating characteristic (ROC) curves were generated per individual metric and the combined model. Input for generation of these ROC curves was the metric associated with each region per patient (357 regions total). We performed fivefold cross-validation with bootstrapping to ascertain viability of metrics used in the predictive model, as well as quantify distribution of accuracy and area under the curve (AUC). A total of 500 iterations, each with fivefold cross-validation were performed, resulting in a total of 2500 tests. Per iteration, five groups of five randomly sampled patients were designated; then per fold, a binary logistic regression model was trained on four groups and tested on the remaining group. Model accuracy and AUC per iteration and fold were used to ascertain distribution of the predictive model.

Statistical analysis was performed with MATLAB, and statistical significance was assessed at $P < .05$. When multiple *t* tests were used to compare values between two groups, we used the Bonferroni-Holm method to correct for multiple comparisons. When ANOVA was used to compare values between more than two groups, we used Tukey's honest significant difference criterion (THSDC) to correct for multiple comparisons.

3 | RESULTS

3.1 | Patient characteristics

For patients in this study, 14.3 ± 4.7 (mean ± standard deviation) brain regions were sampled using 9.5 ± 2.0 electrodes and 106.4 ± 29.3 electrode contacts (Table 1). Overall, each region sampled had 4.4 ± 2.3 electrode contact pairs used for analysis (min = 1, max = 14). The mean stay length in the epilepsy monitoring unit was 9.9 ± 4.2 days. By the end of the clinical SEEG, seizure onset in 18 patients was localized to mesial temporal structures, with 7 individuals experiencing bilateral mesial temporal lobe seizures. In the remaining seven patients, focal neocortical seizure onset was demonstrated.

3.2 | Regions with increased epileptogenicity display higher functional connectivity

We first evaluated connectivity across brain regions in all patients using nondirectional resting-state connectivity measures. With use of a dichotomized regional classification scheme as in prior work,[15] epileptogenic regions demonstrated higher MI strength than nonepileptogenic structures (Figure 1A) ($P = 2.71e\text{-}04$, $t = 4.69$, $df = 24$, paired *t* test, Bonferroni-Holm correction). After reclassifying brain areas in the same patients into four categories of epileptogenicity, we observed that ictogenic regions showed higher MI strength than irritative, or uninvolved structures (Figure 1B) ($P_{\text{total}} = 4.89e\text{-}05$, $P_{\text{ictogenicVSirritative}} = 0.029$, $P_{\text{ictogenicVSuninvolved}} = 1.66e\text{-}05$, $df = 85$, $F = 8.62$, one-way ANOVA with THSDC post hoc). Notably, as in our prior work in a smaller cohort,[15] epileptogenic regions showed higher "between" imaginary coherence (to other brain regions) ($P = 2.55e\text{-}04$, $t = 4.56$, $df = 24$) and "within" imaginary coherence (among electrode contacts within structure) ($P = 2.28e\text{-}03$, $t = 3.41$, $df = 24$, paired *t* test, Bonferroni-Holm correction) compared to nonepileptogenic regions. Using four region classification, ictogenic zones showed higher "between" ($P_{\text{total}} = 1.48e\text{-}05$, $P_{\text{ictogenicVSirritative}} = 0.0022$, $P_{\text{ictogenicVSuninvolved}} = 0.0017$, $df = 85$, $F = 9.72$) and "within" imaginary coherence ($P_{\text{total}} = .0039$, $P_{\text{ictogenicVSuninvolved}} =$

0.039, $df = 85$, $F = 4.80$, one-way ANOVA with THSDC post hoc) than irritative and/or uninvolved regions.

To better visualize variability in connectivity patterns, we examined three-dimensional representations of MI strength in individual patients (Figure 2). Two anecdotal patient cases are shown in Figure 2 and Figure 4. In many patients, ictogenic regions demonstrated higher MI strength than other brain regions, and connectivity of uninvolved and irritative areas was relatively low. This is demonstrated in example Patient 1 with bilateral hippocampal seizures who received bilateral SEEG implantation (Figure 2A). However, MI strength maps in other patients did not show a clear relationship between connectivity and epileptogenicity of brain structures, such as example Patient 2, who had right frontal lobe epilepsy and underwent unilateral implantation (Figure 2B). Patient 2 had uninvolved regions of comparable magnitude to ictogenic regions, and the largest MI strength region was irritative, and overall values in this patient did not follow the general trend observed (Figure 2B). Overall, these results suggest that regions with increased epileptogenicity often demonstrate higher resting-state connectivity using non-directional measures. However, given that these nondirected connectivity patterns vary, exploring additional connectivity metrics may help further improve identification of seizure networks.

3.3 | Ictogenic regions demonstrate higher inward but not outward directed connectivity

We then utilized the directed connectivity measures PDC and DTF to understand whether resting-state functional connectivity increases in seizure-onset regions are more likely driven by inward or outward connections. Using dichotomized region classification, we observed that although epileptogenic structures demonstrated higher PDC inward strength than nonepileptogenic areas ($P = 1.26e\text{-}05$, $t = 6.03$, $df = 24$), PDC outward strength did not differ between regions ($P = 1.00$, $t = -0.55$, $df = 24$, paired t tests, Bonferroni-Holm correction). Similarly, epileptogenic regions showed increased DTF inward strength ($P = 5.84e\text{-}05$, $t = 5.30$, $df = 24$), but not outward strength compared to non-epileptogenic areas ($P = .91$, $t = -0.12$, $df = 24$, paired t tests, Bonferroni-Holm correction). Using four-region classification, ictogenic structures demonstrated higher inward connectivity using PDC (Figure 3A) ($P_{total} = 9.26e\text{-}07$, $P_{ictogenicVSearly\text{-}propagation} = 7.02e\text{-}04$, $P_{ictogenicVSirritative} = 1.14e\text{-}05$, $P_{ictogenicVSuninvolved} = 8.73e\text{-}06$, $df = 85$, $F = 12.38$, one-way ANOVA with THSDC post hoc), did not differ between region types (Figure 3B) ($P = .47$, one-way ANOVA). Likewise, ictogenic areas displayed increased DTF inward strength relative to irritative and uninvolved regions (Figure 3C) ($P_{total} = 0.0029$, $P_{ictogenicVSirritative} = 0.023$, $P_{ictogenicVSuninvolved} = 0.0026$, $df = 85$, $F = 5.05$, one-way ANOVA with THSDC post hoc), but not outward strength (Figure 3D) ($P = .31$, one-way ANOVA) compared to other areas.

We visualized PDC and DTF maps for individual patients, to better appreciate magnitude/directionality of connections. Example PDC and DTF maps for the same two patients in Figure 2 are provided in Figure 4. In the PDC map for example Patient 1, there are several high-magnitude inward connections into ictogenic hippocampi, with a particularly large connection from the right amygdala (early propagation) to the right hippocampus (Figure 4A). A similar, but less-dramatic pattern, is seen in the DTF map for this individual, where ictogenic hippocampi receive primarily inward functional connections (Figure 4B). In

example Patient 2, both PDC (Figure 4C) and DTF (Figure 4D) maps reveal high-magnitude inward connections to ictogenic regions in the frontal lobe, and high connectivity in early propagation areas in the frontal lobe and insula, but not the temporal lobe. Overall, results suggest that seizure-onset regions may demonstrate markedly higher inwarddirected connectivity compared to other regions, and directed connectivity maps may aid in ictogenic structure identification.

3.4 | Connectivity model predicts ictogenicity of individual brain regions

Next we tested a connectivity model combining directed and nondirected measures to help predict whether an individual's brain regions are likely to generate seizures. Based on the results of univariate testing above, we chose MI strength, "between" and "within" imaginary coherence, and PDC and DTF inward strength to incorporate into the model; we also evaluated the predictive value of these individual measures using ROC curves (Figure 5). Among nondirected connectivity measures, nonlinear MI strength demonstrated higher accuracy in predicting ictogenicity (AUC = 0.77) compared to "between" (AUC = 0.68) and "within" imaginary coherence (AUC = 0.64) (Figure 5A). PDC inward strength (AUC = 0.84) showed improved performance over DTF inward strength (AUC = 0.72), and overall displayed highest accuracy of individual measures (Figure 5B). Using logistic regression, combined connectivity model predicted ictogenic regions with an AUC of 0.88 and accuracy of 84.3%, translating to a sensitivity of 79.4% and specificity of 81.9% at maximum sensitivity plus specificity (Figure 5C). Bootstrapping with fivefold cross-validation showed an AUC of 0.89 ± 0.03 and accuracy of 84.7 ± 5.5%. This finding suggests that a connectivity model combining resting-state nondirected and directed connectivity may help identify seizure-onset regions with relatively high accuracy.

3.5 | Connectivity model in patients with favorable seizure outcomes

After SEEG recordings, at the time of analyses, 21 of 25 patients had surgical intervention and ≥12 months of postoperative follow-up (mean: 20.9, range: 12.0–72.0 months). Of these individuals, four underwent frontal lobe resection, seven had selective amygdalohippocampectomy, four received temporal lobectomy, one underwent insular resection, and five received RNS. Of the resection patients (n = 16), the latest seizure outcome was Engel I in nine patients (56.3%), Engel II in four (25.0%), and Engel III in three (18.8%), whereas three (60%) of five who underwent RNS achieved ≥50% decrease in seizure frequency from baseline. We retested the accuracy of our model (Figure 5C) in predicting ictogenicity, restricting analysis to 12 patients who underwent surgery and had favorable seizure outcomes at ≥1 year follow-up (Engel I after resection or ≥50% seizure decrease after RNS). In these patients, the model demonstrated an AUC of 0.93, accuracy of 87.5%, and a sensitivity and specificity of 88.9% and 90.8%, respectively, at maximum sensitivity plus specificity. This suggests that the model performs particularly well in patients within whom we have a higher confidence of seizure onset localization, given favorable postoperative outcomes.

4 | DISCUSSION

Overall, our results suggest that epileptogenic regions demonstrate increased nondirected functional connectivity and higher inward directed connectivity from brief resting-state SEEG recordings, and a model incorporating both directed and nondirected connectivity measures may help identify seizure-onset zones with relatively high accuracy.

4.1 | Nondirected connectivity measures in defining epileptogenicity

Regarding nondirected linear connectivity measures, alpha-band imaginary coherence was higher (a) within epileptogenic areas and (b) between epileptogenic regions than other structures sampled, consistent with our prior study.[15] Other intracranial EEG studies have also found high nondirected connectivity in epileptogenic networks in mesial temporal lobe epilepsy,[39,40] focal neocortical epilepsy,[14] and mixed patient populations.[12] Of interest, we observed larger connectivity increases in epileptogenic regions using information-based nondirected measure, MI strength. We also evaluated connectivity across the four regional categories to further evaluate the epileptic network. Other SEEG connectivity studies have also demonstrated value in separately evaluating early seizure propagation areas.[11,27] Using these classifications, ictogenic regions demonstrated higher MI strength than irritative and uninvolved regions (Figure 1). Finally, MI strength demonstrated improved accuracy in identifying ictogenic structures compared to coherence-based measures (Figure 5A). Overall, clinically useful information about epileptic networks can be garnered using nondirected connectivity measures, and nondirected nonlinear measures particularly deserve further exploration.

4.2 | Directed connectivity patterns in the seizure-onset zone and potential origins

We also evaluated directed connectivity measures, PDC and DTF, to probe directionality of altered functional connections in epileptic networks. Using both directed measures, ictogenic structures demonstrate markedly higher inward but not outward connectivity (Figure 3), and directed connectivity maps in individual patients may aid in epileptic network visualization (eg, Figure 4). Notably, of individual directional measures evaluated, PDC inward strength connectivity demonstrated the highest AUC in predicting ictogenicity (Figure 5B). Higher inward connectivity during the interictal period was also noted in smaller intracranial EEG studies,[41–43] but one study in eight patients observed higher outward connectivity from the ictalonset zone once a seizure starts.[44] It is possible that high resting-state inward connectivity reflects inhibitory input from other regions, to prevent seizure origin/spread, but direction of these signals may flip when seizure activity begins.[45] This hypothesis is further supported by intracranial EEG studies in neocortical epilepsy demonstrating functional isolation of epileptogenic areas at rest,[46,47] or that increased synchronization in seizure-onset regions may be suggestive of an inhibitory surround.[13] It has also been hypothesized that widespread network inhibition seen in temporal lobe epilepsy may have evolved to prevent seizure propagation.[48] Confirmation of this hypothesis may be gained by correlating directed connectivity patterns with measurements of inhibitory/excitatory neurotransmission in animal models.

4.3 | Clinical utility of resting-state SEEG connectivity models

Ultimately, the goal of this work is to improve surgical treatment of focal epilepsy, which depends on accurate delineation of epileptic networks. Our predictive model combining directed and nondirected measures to predict ictogenicity demonstrated relatively favorable performance (AUC = 0.88) and showed somewhat higher accuracy than individual measures (Figure 5C). Ictal interpretation of SEEG has limitations from localization accuracy, medication changes, safety/comfort concerns, and challenges capturing all seizure types during hospitalization.[9,10] One study of bilateral temporal lobe epilepsy patients treated with RNS demonstrated that in approximately one-third of patients, >4 weeks of recordings were required to capture bilateral independent seizures.[49] If validated, this work or similar network analysis of brief resting-state recordings by other groups may help reduce the time a traditional interpretation of SEEG currently takes and thus lead to shorter hospitalizations with fewer interventions to trigger seizures.

4.4 | Limitations and alternatives

One study limitation is that traditional clinical interpretation was used as the “gold-standard” to define epileptogenicity of regions, and these subjective interpretations may be inaccurate. However, in a subset of patients with favorable postoperative seizure outcomes, where confidence in region assignments is higher, connectivity model performance was somewhat improved in predicting ictogenicity (AUC = 0.93 vs 0.88). When data from a larger number of patients with long-term outcomes is available, it will be worthwhile to evaluate the relationship between connectivity and seizure outcome. Our analyses are also limited to regions sampled by SEEG electrodes, and thus may exclude relevant seizure network areas. Future investigations may utilize noninvasive functional neuroimaging techniques to better elucidate the relationship between whole-brain interactions and SEEG connectivity in structures sampled invasively. Next, we utilized only a single 2-minute data segment for our analyses to achieve stable connectivity values, avoid artifact or spike activity, and to create a simple, reproducible model that ultimately can be implemented at other centers. For our methods to be easily implemented in a clinical setting, data from a larger cohort of patients will be needed to define connectivity thresholds more clearly in ictogenic regions and to help predict the probability that an individual brain region is ictogenic. In addition, it will be useful to create an automated pipeline to identify electrode contacts that are positioned within gray matter, and accurately assign electrode contacts to designated brain regions using a coregistered atlas (performed manually in the present study). In future studies, exploring the influence of data segment duration on model fitting, which may further improve connectivity models, may be considered. Finally, although in our current protocol we collect resting-state data on the first day of SEEG study, there was variability in the current cohort, with data collected on day 1.5 ± 1.7 (mean ± standard deviation) across patients. The influence of medications on network connectivity is unknown and may be studied further using serial connectivity measurements.

4.5 | Conclusions

Nondirected and directed connectivity measurements from brief resting-state SEEG recordings may help delineate epileptic regions in patients with focal epilepsy, and a model

incorporating connectivity measures may help predict ictogenicity of individual brain regions. In particular, seizure-onset zones demonstrate markedly elevated inward but not outward connectivity at rest, which may reflect broad inhibitory input to prevent ictal activity. If validated, resting-state connectivity analysis may supplement traditional interpretation of SEEG in focal epilepsy, improving localization accuracy and surgical treatment in this devastating disorder.

ACKNOWLEDGMENTS

The authors thank the patients for their participation. This work was supported in part by National Institutes of Health grants T32 EB001628-17 (SN), F31 NS106735 (HFJG), R21 NS113031 (JDR), K23 NS114178 (JDR), R00 NS097618 (DJE), R01 NS095291 (BMD), and R01 NS112252 (DJE), and the Vanderbilt Institute for Surgery and Engineering (VISE).

Funding information

National Institutes of Health, Grant/Award Number: F31 NS106735, K23 NS114178, R00 NS097618, R01 NS095291, R01 NS112252, R21 NS113031 and T32 EB001628-17

REFERENCES

1. Behr C, Goltzene M, Kosmalski G, Hirsch E, Ryvlin P. Epidemiology of epilepsy. Rev Neurol (Paris). 2016;172(1):27–36. [PubMed: 26754036]
2. Englot DJ, Chang EF. Rates and predictors of seizure freedom in resective epilepsy surgery: an update. Neurosurg Rev. 2014;37(3):389–405. [PubMed: 24497269]
3. Andrews JP, Gummadavelli A, Farooque P, Bonito J, Arencibia C, Blumenfeld H, et al. Association of seizure spread with surgical failure in epilepsy. JAMA Neurol. 2019;76(4):462–9. [PubMed: 30508033]
4. Mullin JP, Shriver M, Alomar S, Najm I, Bulacio J, Chauvel P, et al. Is SEEG safe? A systematic review and meta-analysis of stereo-electroencephalography–related complications. Epilepsia. 2016;57(3):386–401. [PubMed: 26899389]
5. Englot DJ. A modern epilepsy surgery treatment algorithm: incorporating traditional and emerging technologies. Epilepsy Behav. 2018;80:68–74. [PubMed: 29414561]
6. Bancaud J, Dell M. Technics and method of stereotaxic functional exploration of the brain structures in man (cortex, subcortex, central gray nuclei). Rev Neurol (Paris). 1959;101:213–27. [PubMed: 13848920]
7. Abou-Al-Shaar H, Brock AA, Kundu B, Englot DJ, Rolston JD. Increased nationwide use of stereoencephalography for intracranial epilepsy electroencephalography recordings. J Clin Neurosci. 2018;53:132–4. [PubMed: 29724650]
8. Isnard J, Taussig D, Bartolomei F, Bourdillon P, Catenoix H, Chassoux F, et al. French guidelines on stereoelectroencephalography (SEEG). Neurophysiol Clin. 2018;48(1):5–13. [PubMed: 29277357]
9. Rheims S, Ryvlin P. Patients' safety in the epilepsy monitoring unit: time for revising practices. Curr Opin Neurol. 2014;27(2):213–8. [PubMed: 24553465]
10. Karthick P, Tanaka H, Khoo HM, Gotman J. Could we have missed out the seizure onset: a study based on intracranial EEG. Clin Neurophysiol. 2020;131(1):114–26. [PubMed: 31760210]
11. Bettus G, Ranjeva J-P, Wendling F, Bénar CG, Confort-Gouny S, Régis J, et al. Interictal functional connectivity of human epileptic networks assessed by intracerebral EEG and BOLD signal fluctuations. PLoS One. 2011;6(5):e20071. [PubMed: 21625517]
12. Shah P, Bernabei JM, Kini LG, Ashourvan A, Boccanfuso J, Archer R, et al. High interictal connectivity within the resection zone is associated with favorable post-surgical outcomes in focal epilepsy patients. Neuroimage Clin. 2019;23:101908. [PubMed: 31491812]
13. Kini LG, Bernabei JM, Mikhail F, Hadar P, Shah P, Khambhati AN, et al. Virtual resection predicts surgical outcome for drug-resistant epilepsy. Brain. 2019;142(12):3892–905. [PubMed: 31599323]

14. Lagarde S, Roehri N, Lambert I, Trebuchon A, McGonigal A, Carron R, et al. Interictal stereotactic-EEG functional connectivity in refractory focal epilepsies. Brain. 2018;141(10):2966–80. [PubMed: 30107499]
15. Goodale SE, Gonzalez HFJ, Johnson GW, Gupta K, Rodriguez WJ, Shults R, et al. Resting-state SEEG may help localize epileptogenic brain regions. Neurosurgery. 2020;86(6):792–801. [PubMed: 31814011]
16. Rosenow F, Lüders H. Presurgical evaluation of epilepsy. Brain. 2001;124(9):1683–700. [PubMed: 11522572]
17. Bowyer SM. Coherence a measure of the brain networks: past and present. Neuropsychiat Electrophysiol. 2016;2(1):1.
18. Engel J Jr. Outcome with respect to epileptic seizures In: Engel J Jr, editor. Surgical treatment of the epilepsies. New York, NY: Raven Press; 1987 p. 553–71.
19. D'Haese P-F, Pallavaram S, Li R, Remple MS, Kao C, Neimat JS, et al. CranialVault and its CRAVE tools: a clinical computer assistance system for deep brain stimulation (DBS) therapy. Med Image Anal. 2012;16(3):744–53. [PubMed: 20732828]
20. Raichle ME, MacLeod AM, Snyder AZ, Powers WJ, Gusnard DA, Shulman Gl. A default mode of brain function. Proc Natl Acad Sci USA. 2001;98(2):676–82. [PubMed: 11209064]
21. Delorme A, Makeig S. EEGLAB: an open source toolbox for analysis of single-trial EEG dynamics including independent component analysis. J Neurosci Methods. 2004;134(1):9–21. [PubMed: 15102499]
22. Chu CJ, Kramer MA, Pathmanathan J, Bianchi MT, Westover MB, Wizon L, et al. Emergence of stable functional networks in long-term human electroencephalography. J. Neurosci 2012;32(8):2703–13. [PubMed: 22357854]
23. Guggisberg AG, Honma SM, Findlay AM, Dalal SS, Kirsch HE, Berger MS, et al. Mapping functional connectivity in patients with brain lesions. Ann Neurol. 2008;63(2):193–203. [PubMed: 17894381]
24. Oostenveld R, Fries P, Maris E, Schoffelen J-M. FieldTrip: open source software for advanced analysis of MEG, EEG, and invasive electrophysiological data. Comput Intell Neurosci. 2011;2011:1–9. [PubMed: 21837235]
25. Luders HO, Engel JJ, Munari C. General principles In: Engel JJ, editor. Surgical treatment of the epilepsies, 2nd edn. New York, NY: Raven Press; 1993 p. 137–53.
26. Luders HO, Najm I, Nair D, Widdess-Walsh P, Bingman W. The epileptogenic zone: general principles. Epileptic Disord. 2006;8(Suppl 2):S1–9. [PubMed: 17012067]
27. Bartolomei F, Lagarde S, Wendling F, McGonigal A, Jirsa V, Guye M, et al. Defining epileptogenic networks: contribution of SEEG and signal analysis. Epilepsia. 2017;58(7):1131–47. [PubMed: 28543030]
28. Magri C, Whittingstall K, Singh V, Logothetis NK, Panzeri S. A toolbox for the fast information analysis of multiple-site LFP, EEG and spike train recordings. BMC Neurosci. 2009;10(1):81. [PubMed: 19607698]
29. Panzeri S, Magri C, Logothetis NK. On the use of information theory for the analysis of the relationship between neural and imaging signals. Magn Reson Imaging. 2008;26(7):1015–25. [PubMed: 18486395]
30. Xia M, Wang J, He Y. BrainNet Viewer: a network visualization tool for human brain connectomics. PLoS One. 2013;8(7):e68910. [PubMed: 23861951]
31. Rolston JD, Chang EF. Critical language areas show increased functional connectivity in human cortex. Cereb Cortex. 2017;17:1–8.
32. Coito A, Plomp G, Genetti M, Abela E, Wiest R, Seeck M, et al. Dynamic directed interictal connectivity in left and right temporal lobe epilepsy. Epilepsia. 2015;56(2):207–17. [PubMed: 25599821]
33. Adkinson JA, Karumuri B, Hutson TN, Liu R, Alamoudi O, Vlachos I, et al. Connectivity and centrality characteristics of the epileptogenic focus using directed network analysis. IEEE Trans Neural Syst Rehabil Eng. 2018;27(1):22–30. [PubMed: 30561346]

34. Krishnan B, Vlachos I, Wang Z, Mosher J, Najm I, Burgess R, et al. Epileptic focus localization based on resting state interictal MEG recordings is feasible irrespective of the presence or absence of spikes. Clin Neurophysiol. 2015;126(4):667–74. [PubMed: 25440261]
35. Hutson T, Pizarro D, Pati S, Iasemidis LD. Predictability and resetting in a case of convulsive status epilepticus. Front Neurol. 2018;9:172. [PubMed: 29623064]
36. Blinowska KJ. Review of the methods of determination of directed connectivity from multichannel data. Med Biol Eng Compu. 2011;49(5):521–9.
37. Baccalá LA, Sameshima K. Partial directed coherence: a new concept in neural structure determination. Biol Cybern. 2001;84(6):463–74. [PubMed: 11417058]
38. Pagnotta MF, Plomp G. Time-varying MVAR algorithms for directed connectivity analysis: critical comparison in simulations and benchmark EEG data. PLoS One. 2018;13(6):e0198846. [PubMed: 29889883]
39. Karunakaran S, Rollo MJ, Kim K, Johnson JA, Kalamangalam GP, Aazhang B, et al. The interictal mesial temporal lobe epilepsy network. Epilepsia. 2018;59(1):244–58. [PubMed: 29210066]
40. Bartolomei F, Bettus G, Stam CJ, Guye M. Interictal network properties in mesial temporal lobe epilepsy: a graph theoretical study from intracerebral recordings. Clin Neurophysiol. 2013;124(12):2345–53. [PubMed: 23810635]
41. Mao JW, Ye XL, Li YH, Liang P-J, Xu J-W, Zhang P-M. Dynamic network connectivity analysis to identify epileptogenic zones based on stereo-electroencephalography. Front Comput Neurosci. 2016;10:113. [PubMed: 27833545]
42. Vlachos I, Krishnan B, Treiman DM, Tsakalis K, Kugiumtzis D, Iasemidis LD. The concept of effective inflow: application to interictal localization of the epileptogenic focus from iEEG. IEEE Trans Biomed Eng. 2016;64(9):2241–52. [PubMed: 28092511]
43. Li Y-H, Ye X-L, Liu Q-Q, Mao J-W, Liang P-J, Xu J-W. Localization of epileptogenic zone based on graph analysis of stereo-EEG. Epilepsy Res. 2016;128:149–57. [PubMed: 27838502]
44. Van Mierlo P, Carrette E, Hallez H, Raedt R, Meurs A, Vandenberghe S, et al. Ictal-onset localization through connectivity analysis of intracranial EEG signals in patients with refractory epilepsy. Epilepsia. 2013;54(8):1409–18. [PubMed: 23647147]
45. Chakravarthy N, Tsakalis K, Sabesan S, Iasemidis L. Homeostasis of brain dynamics in epilepsy: a feedback control systems perspective of seizures. Ann Biomed Eng. 2009;37(3):565–85. [PubMed: 19125333]
46. Bandt SK, Bundy DT, Hawasli AH, Ayoub KW, Sharma M, Hacker CD, et al. The role of resting state networks in focal neocortical seizures. PLoS One. 2014;9(9):e107401. [PubMed: 25247680]
47. Ibrahim GM, Anderson R, Akiyama T, Ochi A, Otsubo H, Singh-Cadieux G, et al. Neocortical pathological high-frequency oscillations are associated with frequency-dependent alterations in functional network topology. J Neurophysiol. 2013;110(10):2475–83. [PubMed: 24004529]
48. Englot DJ, Blumenfeld H. Consciousness and epilepsy: why are complex-partial seizures complex?. Progress Brain Res. 2009;177:147–70.
49. King-Stephens D, Mirro E, Weber PB, Laxer KD, Van Ness PC, Salanova V, et al. Lateralization of mesial temporal lobe epilepsy with chronic ambulatory electrocorticography. Epilepsia. 2015;56(6):959–67. [PubMed: 25988840]

Key Points

- Nondirectional connectivity is higher in epileptogenic vs nonepileptogenic regions using linear and information-based measures.
- Ictogenic regions demonstrate markedly higher inward but not outward directional connectivity.
- A logistic regression model incorporating connectivity measures predicts ictogenicity of individual regions with an area under the curve (AUC) of 0.88.
- Our study suggests that brief resting-state stereo-electroencephalography (SEEG) data segments may be used to predict seizure-onset zones with reasonable accuracy.

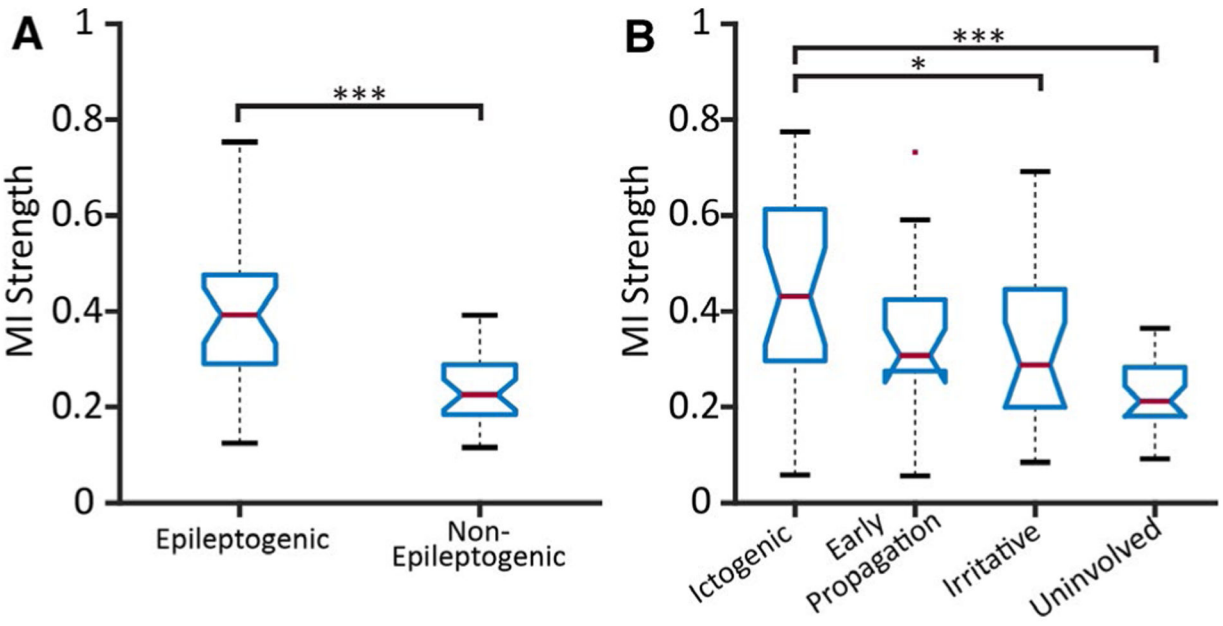

FIGURE 1.

Brain regions with greater epileptogenicity demonstrate higher mutual information (MI) strength. A, MI strength in epileptogenic regions (mean ± standard deviation) (0.40 ± 0.14) is higher than in nonepileptogenic structures (0.24 ± 0.07), using a dichotomized classification scheme of epileptogenicity (paired-sample *t* test). B, MI strength was compared between regions using four categories of epileptogenicity using a one-way analysis of variance (ANOVA) with Tukey's honest significant difference criterion (THSDC) post hoc. MI strength of ictogenic regions (0.45 ± 0.20) was higher than irritative (0.31 ± 0.17) and uninvolved (0.22 ± 0.07) regions. In both panels, the central red line represents the median, and the top and bottom lines indicate the 75th and 25th percentiles, respectively. The red dots represent outliers, and the whiskers visualize the extremes of the data. (N = 25 focal epilepsy patients.) $*P < .05$, $**P < .01$, $***P < .001$ with Bonferroni-Holm correction for multiple comparisons for *t* tests, where applicable

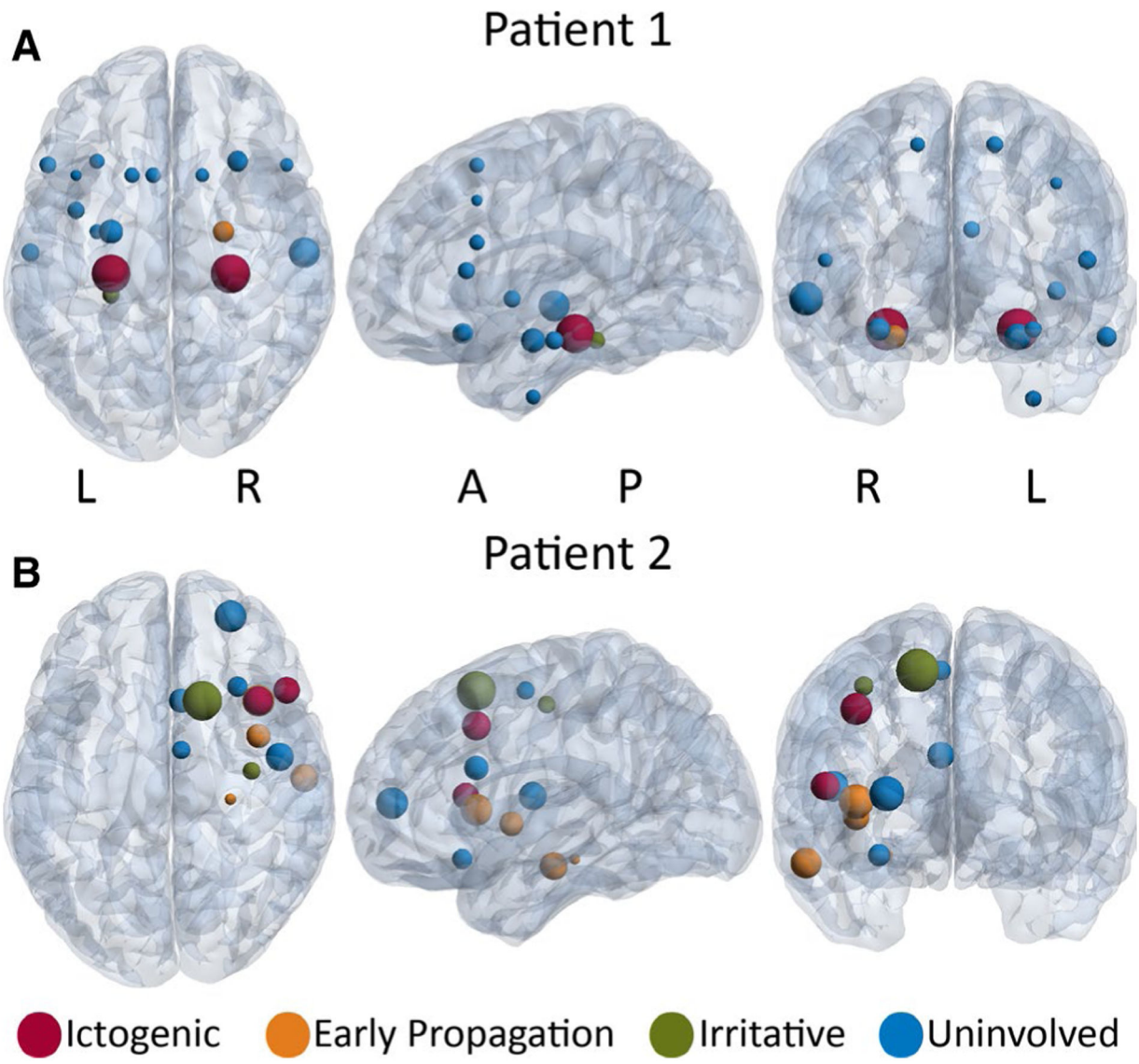

FIGURE 2.

Mutual information (MI) strength maps in two example patients. A, Patient 1 is a right-handed, 29-year-old woman with 8 y duration of epilepsy. The ictogenic regions (red) are the left and right hippocampi. The early propagation region (orange)is the right amygdala, and the irritative region (green) is the left parahippocampal gyrus. In this patient, ictogenic regions demonstrate highest MI strength. B, Patient 2 is a right-handed, 24-year-oldman with 10 y duration of epilepsy. The ictogenic regions (red) are the right inferior frontal gyrus and middle frontal gyrus. The early propagation regions (orange) are the right insula, frontal operculum cortex, hippocampus, and middle temporal gyrus. The irritative regions (green) are the right precentral gyrus and superior frontal gyrus. In this patient, no clear relationship was seen between epileptogenicity and MI strength. In both panels, the size of the spheres is proportional to MI strength of the region. A full list of the regions sampled are listed in Figure 4 legend. A = anterior, L = left, P = posterior, R = right

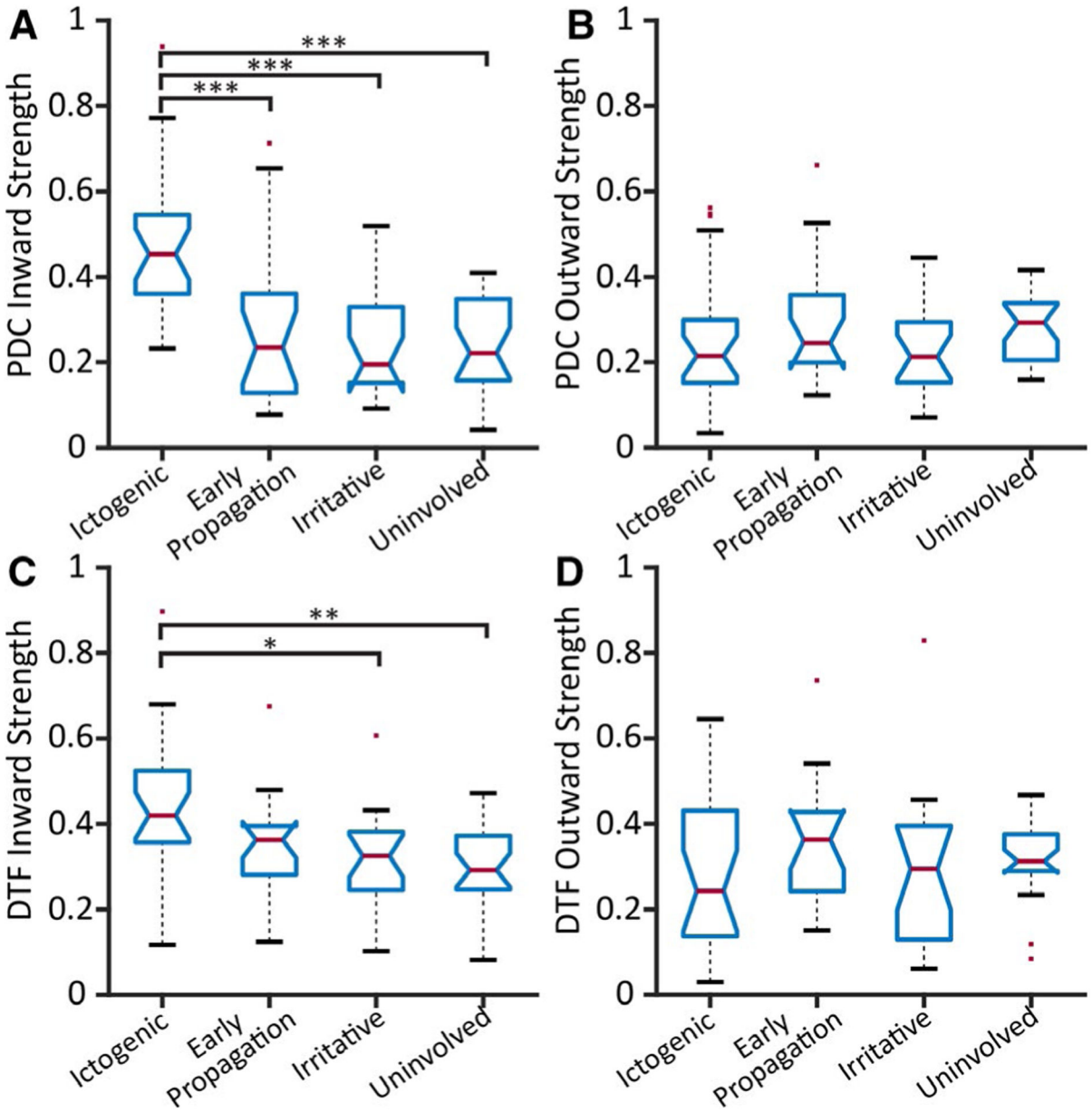

FIGURE 3.

Ictogenic regions demonstrate higher inward but not outward directed connectivity. Strengths of PDC inward (A), PDC outward (B), DTF inward (C), and DTF outward (D) are shown across all patients. Ictogenic regions demonstrate higher inward strength (A, C) but not outward strength (B, D) using both directed connectivity measures. The PDC inward strength values (mean ± standard deviation) are: ictogenic (0.47 ± 0.17), early propagation (0.28 ± 0.19), irritative (0.24 ± 0.12), and uninvolved (0.25 ± 0.11). The DTF inward strength values are: ictogenic (0.43 ± 0.16), early propagation (0.35 ± 0.12), irritative (0.32 ± 0.11), and uninvolved (0.30 ± 0.10). In all four panels, the central red line represents the median, and the top and bottom lines indicate the 75th and 25th percentiles, respectively. The red dots represent outliers, and the whiskers visualize the extremes of the data. (N = 25

patients.) *$P < .05$, **$P < .01$, ***$P < .001$, one-way ANOVA with THSDC post hoc. DTF = directed transfer function, PDC = partial directed coherence

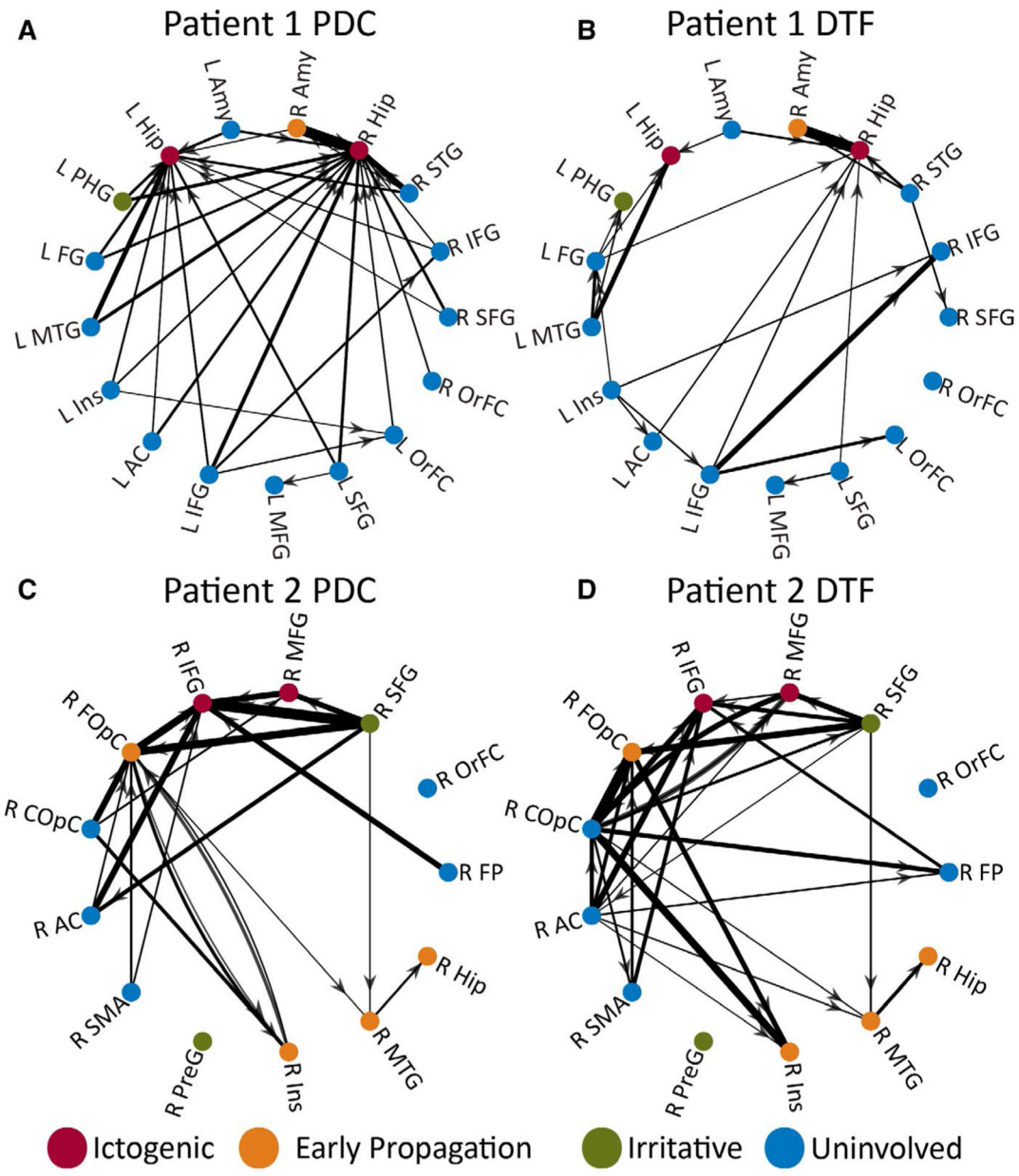

FIGURE 4.

Directed connectivity maps in two example patients. PDC matrices (A, C) and the DTF matrices(B, D) are shown in two example patients, where arrows represent the directionality of the connection and line thickness is proportional to thresholded, rescaled PDC and DTF values. In both patients, structures with greater epileptogenicity, particularly ictogenic regions, demonstrated a larger number of high-magnitude inward connections compared to uninvolved areas. Patients1 and 2 correspond to the same patients shown in Figure 2. R = right, L = left; AC = anterior cingulate gyrus, Amy = amygdala, COpC = central operculum cortex, DTF = directed transfer function, FG = anterior temporal fusiform gyrus, FOpC = frontal operculum cortex, FP = frontal pole, Hip = hippocampus, IFG = inferior frontal gyrus, Ins = insular cortex, MFG = middle frontal gyrus, MTG = middle temporal gyrus,

OrFC = frontal orbital cortex, PDC = partial directed coherence, PHG = parahippocampal gyrus, PreG = precentral gyrus, SFG = superior frontal gyrus, SMA = supplementary motor area, STG = superior temporal gyrus

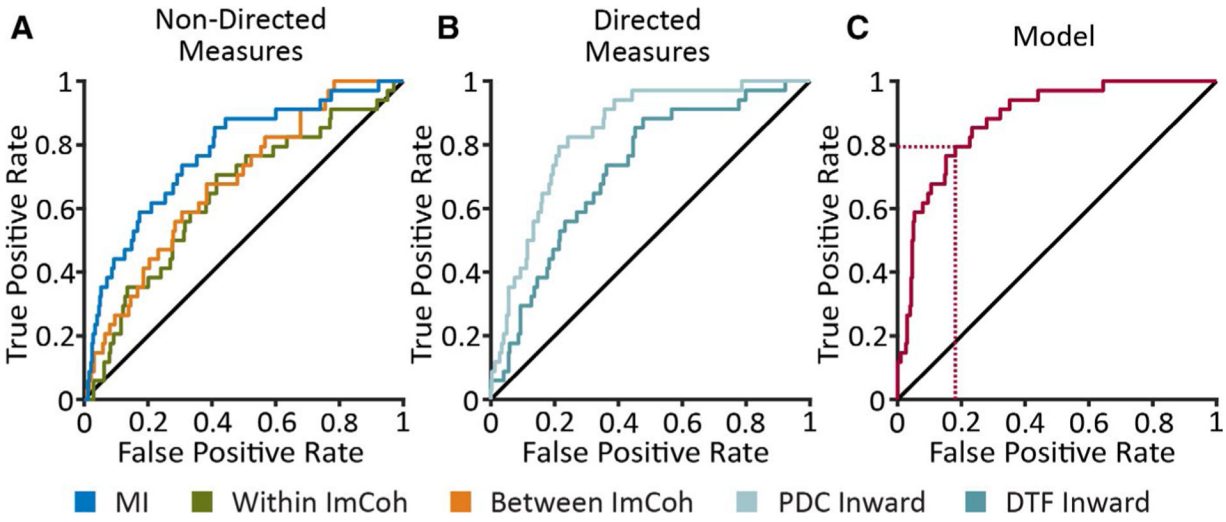

FIGURE 5.

A model incorporating directed and nondirected connectivity measures may help predict ictogenicity of individual brain regions. Receiver-operating characteristic (ROC) curves demonstrate the true-positive and false-positive rates in predicting ictogenicity of 357 total individual brain regions across all 25 patients. Five individual connectivity measures (A, B) and a model (C) that combines these measures with a binary logistic regression analysis are shown. The area under the curve (AUC) values of the nondirected measures (A) varies between 0.64 and 0.77. The AUC values for PDC inward strength and DTF inward strength (B) are 0.84 and 0.72, respectively. The AUC for the summary model (C) is 0.88. The dotted red lines indicate the sensitivity (79.4%) and specificity (81.9%) of the model in predicting ictogenic vs nonictogenic brain regions at maximum sensitivity plus specificity. DTF = directed transfer function, ImCoh = imaginary coherence (alpha-band), PDC = partial directed coherence

TABLE 1

Summary of patient characteristics

Demographics	
Age, years	34.8 ± 11.6
Gender, female	14.0 (56.0)
Handedness, left	8.0 (32.0)
Details of recordings	
Regions sampled	14.3 ± 4.7
Electrodes implanted	9.5 ± 2.0
Electrode contacts implanted	106.4 ± 29.3
Time between beginning SEEG study and resting-state recording, days	1.5 ± 1.7
Electrode contact pairs per region	4.4 ± 2.3
Disease variables	
Epilepsy duration, years	18.8 ± 13.7
Focal aware seizures, monthly	5.3 ± 12.2
Focal impaired awareness seizures, monthly	14.0 ± 35.7
Focal to bilateral tonic-clonic seizures, monthly	1.0 ± 2.4
Seizure-onset region	
Unilateral mesial temporal	11.0 (44.0)
Bilateral mesial temporal	7.0 (28.0)
Focal neocortical	7.0 (28.0)

Note: N = 25. Data are number (%) of patients for categorized variables and mean ± standard deviation for continuous variables.